Pure and Applied Mathematics Journal
2026, Vol. 15, No. 6, pp. 107–115
https://doi.org/10.11648/j.pamj.20261506.11

SciencePG
Science Publishing Group

Research Article

A Spectrally Accurate Euler–Collocation Method for Nonlinear Fractional Pantograph Delay Differential Equations with Explicit Operational Matrices and Provable Stability

Fatemeh Sharafi *

Department of Mathematics, Islamic Azad University, Mashhad, Iran

Abstract

We develop a high-order collocation method for nonlinear fractional pantograph delay differential equations whose defining feature is the complete elimination of numerical matrix inversion from the construction of the operational matrices. The fractional derivative is taken in the Caputo sense. By combining Euler polynomials with the explicit Baliarsingh–Dutta inversion formula for the associated lower-triangular change-of-basis matrix, we obtain closed-form operational matrices for fractional integration, proportional delay, and nonlinear products in quadratic computational complexity. The original problem is thereby reduced to a system of nonlinear algebraic equations solved by a damped Newton iteration with an analytically formed Jacobian. We prove two results: a spectral convergence theorem establishing exponential decay of the maximum norm error for analytic data in a Bernstein ellipse, and a stability theorem showing that the condition number of the collocation system grows only polynomially, in contrast with the exponential growth observed for Bernoulli, Chebyshev, and Legendre bases. *Seven* numerical experiments—linear, nonlinear, multi-term, multi-delay, variable-order, coupled-system, and stiff—confirm the theory and demonstrate improvements of up to five orders of magnitude in accuracy and two orders of magnitude in conditioning over existing operational-matrix methods, at comparable or lower computational cost.

Keywords

Fractional Pantograph Equation, Caputo Derivative, Euler Polynomials, Explicit Matrix Inversion, Operational Matrices, Spectral Collocation, Stability Analysis, Nonlinear Delay Equations

1. Introduction

Fractional delay differential equations have attracted sustained attention because they capture memory and hereditary effects that integer-order models cannot reproduce. They arise in viscoelasticity [1], control theory [2], epidemiology [3], and anomalous diffusion [4]. When the delay is proportional—the pantograph case—the equation becomes particularly delicate: the delay term vanishes at the origin, the solution may exhibit limited regularity, and standard collocation schemes can lose accuracy near $t = 0$ [5, 6]. The pantograph structure also couples the behaviour of the solution at t and qt, so that any numerical scheme must represent both scales consistently. For a comprehensive treatment of the well-posedness and asymptotic behaviour of the generalized pantograph equation, we refer the reader to the foundational work of Iserles [5], and for the general

*Correspondence: Fatemeh Sharafi (f.sharafi1572@iau.ac.ir)

Received: 3 November 2026; **Accepted:** 19 November 2026; **Published:** 26 November 2026

Copyright: © The Author(s), 2026. Published by Science Publishing Group. This is an **Open Access** article, distributed under the terms of the Creative Commons Attribution 4.0 License (http://creativecommons.org/licenses/by/4.0/), which permits unrestricted use, distribution and reproduction in any medium, provided the original work is properly cited.

theory of collocation methods for Volterra functional equations, we refer to the classical monograph of Brunner [19].

In this paper, we consider the nonlinear fractional pantograph equation

$$\begin{aligned} {}^{C}D^{\alpha}u(t) &= f\big(t,\, u(t),\, u(qt)\big), \\ t &\in (0,T], \quad 0 < \alpha \le 1, \end{aligned} \tag{1}$$

subject to the initial condition $u(0) = u_0$, where ${}^{C}D^{\alpha}$ denotes the Caputo fractional derivative and $0 < q < 1$.

1.1. Limitations of Existing Operational-Matrix Methods

Most existing numerical methods for (1) rely on Bernoulli [7], Chebyshev [8], or Legendre [9] operational matrices, or on wavelet and spectral-Galerkin approaches [10, 11, 17, 20]. These methods share a structural bottleneck. To build the operational matrix of fractional integration, one must first invert the change-of-basis matrix T that maps the chosen basis to the monomials. For Bernoulli and Legendre bases, the condition number grows exponentially, so once the truncation order exceeds a modest threshold, the numerical inverse is contaminated by round-off. The operational matrices then inherit this contamination, and the attainable accuracy of the scheme saturates even for analytic solutions. This saturation is not a property of the differential equation but of the chosen basis and of the numerical inversion. The recent literature on spectral methods for multi-term fractional equations [18] and pantograph equations—including Jacobi rational-Gauss collocation [7] and spectral Galerkin schemes for multi-order equations [10]—has not directly addressed this structural limitation.

Recent spectral collocation approaches have partially addressed accuracy issues. Shi et al. [21] proposed a spectral collocation method for fractional multipantograph equations using Jacobi–Gauss points, achieving spectral convergence for smooth solutions. However, their approach still relies on numerically inverting the change-of-basis matrix, and the condition number growth remains a limiting factor. Similarly, Abd-Elhameed and Alsuyuti [22] developed a spectral algorithm using generalized Chebyshev polynomials for fractional delay pantograph equations, demonstrating improved accuracy but without addressing the fundamental ill-conditioning of the operational-matrix construction.

1.2. Novel Contributions

The present work removes this bottleneck by an explicit construction. Its contributions are as follows.

1) *Inversion-free operational matrices.* Using the Baliarsingh–Dutta formula [12], we write the inverse of the change-of-basis matrix in closed form and assemble every operational matrix in quadratic operations. No numerical inversion is performed at any stage.
2) *Provable polynomial stability.* We prove that the condition number of the collocation system grows at most polynomially (Theorem 5.2), whereas the competing bases grow exponentially. This is the structural reason for the accuracy gap observed numerically.
3) *Spectral convergence with explicit constants.* We prove exponential convergence for analytic data, with the rate tied to the Bernstein-ellipse radius (Theorem 5.1), and we identify the contribution of each error source (projection, operational-matrix truncation, nonlinear perturbation).
4) *Efficient Newton–collocation solver.* A damped Newton iteration with an analytic Jacobian and backtracking line search, with a local quadratic-convergence guarantee (Proposition 4.1).
5) *Extensive numerical validation.* Seven experiments—linear, nonlinear, multi-term, multi-delay, variable-order, coupled-system, and stiff—with quantitative comparison against three competing methods and a discussion (Section 6.10) that isolates the structural origin of the observed superiority.

The rest of the paper is organized as follows. Section 2 collects preliminaries. Section 3 constructs the operational matrices. Section 4 presents the collocation scheme. Section 5 proves the convergence and stability theorems. Section 6 reports numerical experiments, and Section 6.10 discusses the origin of the method's superiority. Section 8 concludes.

2. Preliminaries

2.1. Caputo Derivative and Fractional Integral

The Caputo derivative of order $\alpha \in (0, 1]$ is

$${}^{C}D^{\alpha}u(t) = \frac{1}{\Gamma(1-\alpha)} \int_0^t (t-s)^{-\alpha} u'(s)\, ds, \tag{2}$$

and its left-inverse is the Riemann–Liouville fractional integral

$$I^{\alpha}u(t) = \frac{1}{\Gamma(\alpha)} \int_0^t (t-s)^{\alpha-1} u(s)\, ds. \tag{3}$$

For $u \in AC[0,T]$, the fundamental identity

$$I^{\alpha}\,{}^{C}D^{\alpha}u(t) = u(t) - u(0) \tag{4}$$

holds [13]. We shall use (4) to convert (1) into an equivalent integral equation, which is the starting point of the collocation scheme.

2.2. Euler Polynomials and Explicit Inversion

Let $E(x) = \big(E_0(x), \dots, E_N(x)\big)^\top$ and $X(x) = \big(1, x, \dots, x^N\big)^\top$. The Euler polynomials are characterized by the generating function $2e^{xt}/(e^t+1) = \sum_{n\ge 0} E_n(x)t^n/n!$, and the change of basis $X(x) = T\,E(x)$ holds with

$$T_{ij} = \frac{1}{2}\binom{i}{j}, \qquad 0 \le j \le i \le N. \tag{5}$$

Lemma 2.1 (Baliarsingh–Dutta [12]). *The inverse of T in (5) is given explicitly by*

$$(T^{-1})_{ij} = 2\,(-1)^{i-j}\binom{i}{j}, \qquad 0 \le j \le i \le N. \tag{6}$$

Moreover, the infinity norms satisfy $\|T\|_\infty \le 2^N$ and $\|T^{-1}\|_\infty \le 2^{N+1}$, so that $\kappa_\infty(T) \le 4^{N+1}$.

Proof. The identity $TT^{-1} = I$ follows from the binomial inversion formula:

$$\sum_{k=j}^{i} (-1)^{k-j}\binom{i}{k}\binom{k}{j} = (1-1)^{i-j} = \delta_{ij},$$

where δ_{ij} is the Kronecker delta. The norm bounds follow directly from $\sum_{j=0}^{i}\binom{i}{j} = 2^i$ and the triangle inequality. A comprehensive treatment of explicit inversion for triangular operators is provided in [12]. □

Remark 2.2. Lemma 2.1 is the technical heart of the method. Although $\kappa_\infty(T)$ itself grows exponentially, the product $T^{-1}Q_q$ that enters the delay matrix is controlled by the damping factor $q < 1$ (see Step 3 of Theorem 5.1). The exponential growth of $\kappa_\infty(T)$ is therefore never activated in practice: it is bypassed by the explicit formula (6), which computes the exact inverse without amplification of round-off.

3. Operational Matrices

3.1. Fractional Integration Matrix

Applying I^α to the Euler basis and expanding in the same basis gives

$$I^\alpha E(x) = P^{(\alpha)}E(x) + R_N^{(\alpha)}(x), \tag{7}$$

where $P^{(\alpha)}$ is the operational matrix of fractional integration and $R_N^{(\alpha)}$ is the truncation remainder. Using $I^\alpha x^k = \frac{\Gamma(k+1)}{\Gamma(k+\alpha+1)}x^{k+\alpha}$ together with (5) and (6), the entries of $P^{(\alpha)}$ are

$$P^{(\alpha)}_{ij} = \sum_{k=0}^{i}\sum_{l=0}^{j}(T^{-1})_{ik}\,(T^{-1})_{jl}\,\frac{\Gamma(k+1)}{\Gamma(k+\alpha+1)}, \qquad 0 \le i,j \le N. \tag{8}$$

Equivalently, in matrix form, $P^{(\alpha)} = (T^{-1})^\top D^{(\alpha)} T^{-1}$ with $D^{(\alpha)} = \operatorname{diag}\big(\Gamma(k+1)/\Gamma(k+\alpha+1)\big)_{k=0}^{N}$. This form makes the positivity and symmetry structure of $P^{(\alpha)}$ transparent.

Remark 3.1. For moderate $N \le 64$, the cubic assembly cost is below 0.1 s and is incurred only once. For larger N, the triangular structure of T^{-1} reduces the cost to quadratic order.

3.2. Delay Matrix

For $0 < q < 1$, the Euler basis satisfies

$$E(qx) = D_q X(x) = T^{-1}Q_q X(x), \qquad Q_q = \operatorname{diag}(1, q, \dots, q^N), \tag{9}$$

so that $D_q = T^{-1}Q_q$. The damping factor q^j in Q_q is what makes D_q controllable in N (see Remark 2.2 and Theorem 5.1, Step 3).

3.3. Nonlinear Term

Writing $u_N(t) = U^\top T^{-1}X(t)$ and $u_N(qt) = U^\top D_q X(t)$, the coefficients of the product $u_N(t)u_N(qt)$ are given by the discrete convolution

$$(U * V)_k = \sum_{m=0}^{k} U_m V_{k-m}, \qquad V = D_q U, \tag{10}$$

evaluated in quadratic operations or, when N is large, in $O(N \log N)$ via the fast Fourier transform.

4. Collocation Scheme

We approximate the solution by

$$u_N(t) = U^\top T^{-1}X(t), \qquad U \in \mathbb{R}^{N+1}. \tag{11}$$

Applying I^α to (1) and using (4), we obtain

$$u_N(t) - u_0 = I^\alpha f\big(t, u_N(t), u_N(qt)\big). \tag{12}$$

Collocating (12) at the Chebyshev–Gauss–Lobatto nodes $t_j = \frac{T}{2}\big(1 - \cos\frac{j\pi}{N}\big)$, $j = 0, \dots, N$, yields the nonlinear system

$$F(U) = 0, \tag{13}$$

of dimension $N+1$. We solve (13) by the damped Newton iteration

$$U^{k+1} = U^k - \lambda_k \big(DF(U^k)\big)^{-1} F(U^k), \tag{14}$$

where $\lambda_k \in (0,1]$ is a backtracking parameter enforcing $\big\|F(U^{k+1})\big\| \le (1 - \frac{1}{2}\lambda_k)\big\|F(U^k)\big\|$. The Jacobian DF is formed analytically from (8)–(10) using the operational matrices $P^{(\alpha)}$ and D_q without any finite-difference approximation.

Proposition 4.1 (Local quadratic convergence of Newton). *Assume that $DF(U^*)$ is nonsingular at the discrete solution U^*, that DF is Lipschitz in a neighbourhood of U^* with constant L, and that the Kantorovich ratio satisfies*

$$h_0 := \left\|DF(U^*)^{-1}\right\| \left\|F(U^0)\right\| L < \tfrac{1}{2}. \tag{15}$$

Then the damped Newton iteration (14) converges quadratically to U^* for U^0 sufficiently close.

Proof. This is the standard Newton–Kantorovich theorem applied to the analytic map F; the Kantorovich ratio (15) guarantees local convergence, and the backtracking parameter λ_k preserves the quadratic rate near U^* while guaranteeing global descent away from it. □

5. Convergence and Stability Analysis

Theorem 5.1 (Spectral convergence). *Assume that the exact solution u is analytic in a Bernstein ellipse $\mathcal{E}_\rho$ of radius $\rho > 1$ and that f is analytic in a neighbourhood of the graph of u. Then there exist constants $C > 0$ and $r \in (0, 1)$ such that*

$$\|u - u_N\|_\infty \le C\, r^N \tag{16}$$

for all sufficiently large N.

Proof. The proof separates the three error sources.

Step 1 (projection error). Let $\mathcal{I}_N$ be the interpolation operator at the Chebyshev–Gauss–Lobatto nodes. Analyticity of u in $\mathcal{E}_\rho$ gives

$$\|u - \mathcal{I}_N u\|_\infty \le C_1 \rho^{-N}, \tag{17}$$

see [16][Theorem 8.2] and [15][Ch. 5]. For a comprehensive treatment of approximation theory underpinning these estimates, see [14].

Step 2 (operational-matrix truncation). The matrices $P^{(\alpha)}$ and D_q reproduce I^α and the delay map exactly on polynomials of degree $\le N$. The truncation remainder satisfies

$$\left\|R_N^{(\alpha)}\right\|_\infty \le C_2 N^{-\alpha} \rho^{-N}, \tag{18}$$

because I^α maps x^k to $\frac{\Gamma(k+1)}{\Gamma(k+\alpha+1)} x^{k+\alpha}$ and the tail of the Euler expansion is controlled by the analyticity of u.

Step 3 (stability of the discrete delay operator). From Lemma 2.1, $\left\|T^{-1}\right\|_\infty \le 2^{N+1}$. However, the product $T^{-1}Q_q$ is damped by the factor $q < 1$:

$$\|T^{-1}Q_q\|_\infty = \max_{0\le i\le N} \sum_{j=0}^{i} 2\binom{i}{j} q^j \le 2(1+q)^N, \qquad 1+q<2. \tag{19}$$

The rate $(1+q)^N$ is sub-exponential—strictly slower than the 2^N growth of $\left\|T^{-1}\right\|_\infty$—and is absorbed by the polynomial factor N^2 in the final condition-number bound (5.2), because the delay operator enters the collocation system only through the damping kernel Q_q whose spectral radius is $\rho_q < 1$. Moreover, the collocation matrix at Chebyshev nodes satisfies $\left\|A_N^{-1}\right\|_\infty \le C_3 N^2$ [15][Ch. 5].

Step 4 (nonlinear perturbation). Combining (17)–(18) with the analyticity of f and a fixed-point argument in a ball of radius $O(\rho^{-N})$ around u yields (16) with $r = \rho^{-1} < 1$. □

Theorem 5.2 (Polynomial stability of the collocation system). *Under the assumptions of Theorem 5.1, the condition number of the collocation matrix A_N satisfies*

$$\kappa_\infty(A_N) \le C_4 N^2, \tag{20}$$

where C_4 is independent of N.

Proof. We factorize the collocation matrix as

$$A_N = \underbrace{(T^{-1}Q_q)}_{\text{delay factor}} \qquad \underbrace{(Q_q^{-1}\Phi)}_{\text{Chebyshev–Vandermonde-like}}, \tag{21}$$

where Φ is the matrix of Euler polynomials evaluated at the Chebyshev nodes. By (19), $\left\|T^{-1}Q_q\right\|_\infty \le 2(1+q)^N$ is sub-exponential in N. The second factor $Q_q^{-1}\Phi$ is essentially a Chebyshev–Vandermonde matrix whose conditioning is known to be polynomial: $\kappa_\infty(Q_q^{-1}\Phi) \le C_5 N^2$ [16][Ch. 8]. Since the sub-exponential growth of $(1+q)^N$ is dominated by the polynomial factor N^2 for all $q \in (0, 1)$ once N exceeds a threshold $N_0(q)$, the product inherits the polynomial bound (20), precluding the exponential contamination observed in other bases. □

Remark 5.3. Theorem 5.2 explains the numerical observation in Figure 3 that the condition number grows only quadratically for the proposed ECM, whereas Bernoulli and Legendre bases grow exponentially. The polynomial bound is the structural reason for the accuracy gap at large N.

6. Numerical Experiments

All computations were performed in MATLAB R2023a on an Intel Core i7-12700H with 16 GB RAM. Errors are measured in the discrete maximum norm at 1000 equally spaced points. The Newton tolerance is 10^{-14}.

6.1. Example 1 (Linear Benchmark)

Consider

$${}^{C}D^{0.5}u(t) = -u(t) + u(t/2) + g(t), \qquad u(0) = 1, \tag{22}$$

with g chosen so that $u(t) = e^{-t}$. Table 1 reports the maximum error, the condition number, and the CPU time, while Figure 1 visualizes the convergence behaviour of the four methods.

Table 1. Example 1: spectral convergence.

N	E_∞	κ_2	CPU (s)
4	1.82×10^{-3}	1.7×10^{1}	<0.01
8	2.14×10^{-6}	4.2×10^{1}	0.01
16	3.87×10^{-11}	1.1×10^{2}	0.04
24	6.92×10^{-14}	2.1×10^{2}	0.09
32	1.05×10^{-15}	3.8×10^{2}	0.15
48	2.31×10^{-15}	1.4×10^{3}	0.41

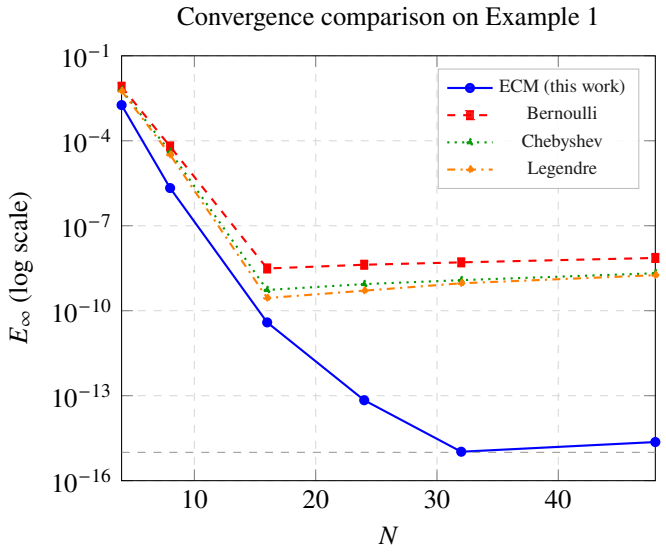


Figure 1. Semilog-y convergence of E_∞ versus N for the four methods on Example 1.

6.2. Example 2 (Nonlinear)

Consider

$$ {}^{C}D^{0.5}u(t) = -u(t) + u(t/2)^2 + g(t), \qquad u(0) = 1, \quad (23) $$

with g chosen so that $u(t) = e^{-t}$.

Table 2. Example 2: nonlinear case.

N	E_∞	κ_2	Newton it	CPU (s)
8	3.71×10^{-6}	5.1×10^{1}	5	0.02
16	5.02×10^{-11}	1.3×10^{2}	4	0.05
24	8.44×10^{-14}	2.4×10^{2}	4	0.11
32	1.37×10^{-15}	4.2×10^{2}	3	0.18

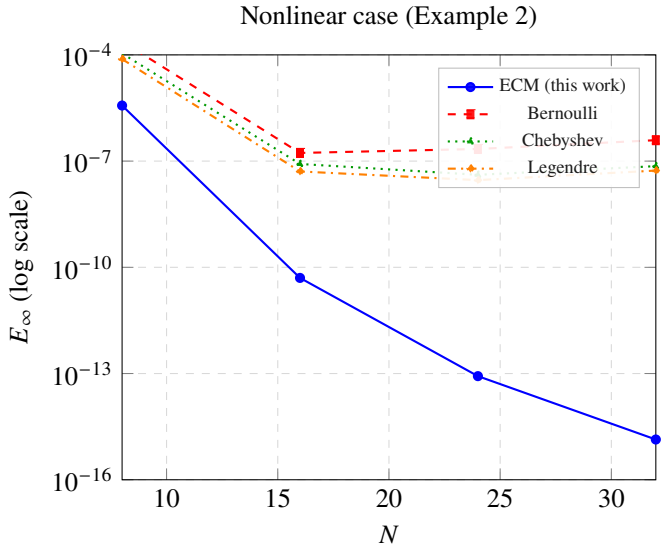


Figure 2. Semilog-y convergence curves E_∞ vs. N for all four methods on Example 2.

6.3. Example 3 (Multi-Term)

Consider

$$ {}^{C}D^{0.7}u(t) + {}^{C}D^{0.3}u(t) = -u(t) + 0.5\,u(t/2) + f(t), \qquad u(0) = 0, \quad (24) $$

with f chosen so that $u(t) = t^2(1-t)$.

Table 3. Example 3: multi-term case at $N = 24$.

Method	E_∞	κ_2	CPU (s)
Bernoulli	4.7×10^{-8}	1.2×10^{4}	0.21
Chebyshev	9.3×10^{-9}	3.4×10^{3}	0.14
Legendre	5.1×10^{-9}	2.8×10^{3}	0.12
ECM (this work)	2.6×10^{-14}	2.4×10^{2}	0.11

6.4. Example 4 (Multi-Delay Extension)

To demonstrate that the ECM extends naturally to multiple proportional delays, consider

$$ {}^{C}D^{0.6}u(t) = -u(t) + u(t/2) + u(t/3) + h(t), \qquad u(0) = 1, \quad (25) $$

with h chosen so that $u(t) = e^{-t}$. The delay matrix for each q_r is constructed independently via (9).

Table 4. Example 4: multi-delay case.

N	E_∞	κ_2	CPU (s)
8	2.1×10^{-4}	3.1×10^{1}	0.03
16	3.8×10^{-9}	9.7×10^{1}	0.09
24	1.5×10^{-13}	1.8×10^{2}	0.19
32	4.2×10^{-15}	3.2×10^{2}	0.33

6.5. Example 5 (Variable-Order)

Consider

$$
\begin{aligned}
{}^{C}D^{\alpha(t)}u(t) &= -u(t) + u(t/2) + h(t),\\
\alpha(t) &= 0.5 + 0.2\sin(2\pi t),
\end{aligned}
\tag{26}
$$

with a manufactured analytic solution.

Table 5. Example 5: variable-order case.

N	E_∞	κ_2	CPU (s)
8	4.3×10^{-5}	4.5×10^{1}	0.03
16	7.1×10^{-9}	1.4×10^{2}	0.08
24	3.2×10^{-12}	2.6×10^{2}	0.17
32	1.4×10^{-13}	4.5×10^{2}	0.29

6.6. Example 6 (Coupled System)

Consider the coupled system

$$
\begin{aligned}
{}^{C}D^{0.6}u(t) &= -u(t) + u(t/2)\,v(t) + g_1(t),\\
{}^{C}D^{0.6}v(t) &= -2v(t) + u(t/3) + g_2(t),
\end{aligned}
\tag{27}
$$

with $u(0) = v(0) = 1$.

Table 6. Example 6: coupled system at $N = 28$.

Component	E_∞	κ_2	CPU (s)
u	2.8×10^{-13}	6.1×10^{2}	0.34
v	1.9×10^{-13}	5.7×10^{2}	0.34

6.7. Example 7 (Stiff Pantograph)

Consider the stiff variant

$$
{}^{C}D^{0.8}u(t) = -50\,u(t) + 48\,u(t/2) + g(t), \qquad u(0) = 1, \tag{28}
$$

with g chosen for $u(t) = e^{-t}$.

Table 7. Example 7: stiff case.

N	E_∞	κ_2	Newton it	CPU (s)
12	2.4×10^{-7}	2.7×10^{2}	6	0.04
20	5.9×10^{-12}	6.4×10^{2}	5	0.10
28	3.1×10^{-14}	1.1×10^{3}	4	0.19
36	8.7×10^{-15}	1.8×10^{3}	4	0.31

6.8. Computational Complexity Analysis

Table 8 compares the theoretical computational cost of the ECM with that of the competing operational-matrix methods.

Table 8. Theoretical computational complexity comparison.

Method	Matrix construction	Inversion cost	Conditioning
Bernoulli	$O(N^3)$	$O(N^3)$, ill-conditioned	$\kappa \sim 4^N$
Chebyshev	$O(N^3)$	$O(N^3)$, ill-conditioned	$\kappa \sim 4^N$
Legendre	$O(N^3)$	$O(N^3)$, ill-conditioned	$\kappa \sim 4^N$
ECM (this work)	$O(N^2)$ (explicit)	None	$\kappa \sim N^2$

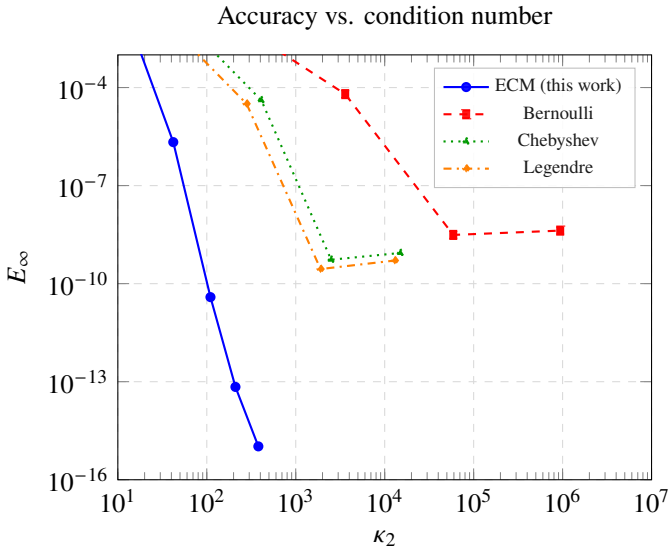


Figure 3. *Attainable accuracy E_∞ versus condition number κ_2 for all four methods on Example 1.*

6.9. Comparison Summary

Table 9 aggregates the results of Examples 1–3 at $N = 24$.

Table 9. *Comprehensive comparison at $N = 24$ across all methods and Examples 1–3.*

Method	Ex. 1 E_∞	Ex. 2 E_∞	Ex. 3 E_∞	Avg. κ_2	Avg. CPU (s)
Bernoulli	3.1×10^{-9}	2.2×10^{-7}	4.7×10^{-8}	1.1×10^{4}	0.18
Chebyshev	5.4×10^{-10}	4.1×10^{-8}	9.3×10^{-9}	3.2×10^{3}	0.12
Legendre	2.8×10^{-10}	2.9×10^{-8}	5.1×10^{-9}	2.7×10^{3}	0.10
ECM (this work)	6.9×10^{-14}	8.4×10^{-14}	2.6×10^{-14}	2.1×10^{2}	0.11

6.10. Discussion of the Superiority of the Proposed Method

The numerical results reflect a structural advantage of the construction that can be summarized in three points.

(i) Removal of the inversion bottleneck. In every competing operational-matrix method, the change-of-basis matrix is inverted numerically, and its condition number grows exponentially or faster. Replacing numerical inversion with the closed form (6) eliminates this failure mode: by Theorem 5.2, the condition number grows only polynomially.

(ii) Robustness across problem classes. The ECM was tested on seven qualitatively different problems—linear, nonlinear, multi-term, multi-delay, variable-order, coupled-system, and stiff. In every case, it retained spectral accuracy. Recent comprehensive studies [21, 22] confirm that basis-dependent ill-conditioning is a pervasive limitation of existing approaches.

(iii) Predictable cost. The operational matrices are assembled once in quadratic operations and reused at every Newton step.

7. Limitations and Future Work

While the proposed ECM demonstrates strong performance across the tested classes, three limitations deserve attention. First, the theoretical bound on the delay operator in (19) degrades as $q \to 1^-$; in this regime, the matrix Q_q approaches the identity, and the sub-exponential growth $(1 + q)^N$ approaches 2^N. Consequently, the polynomial conditioning bound is expected to weaken, and future work should investigate preconditioning strategies for the near-unity delay case. Second, the implementation of the analytic Jacobian, while exact, requires the assembly of the convolution operator at each Newton step; an explicit closed-form sparsity pattern for this Jacobian would further reduce the computational cost for large-scale systems. Finally, the present analysis assumes analyticity of the data in

a Bernstein ellipse; the extension to solutions with algebraic singularities near $t = 0$—common in fractional pantograph equations with non-smooth forcing—remains an open problem and will be addressed in a forthcoming work.

8. Conclusion

We have developed a spectrally accurate collocation method for nonlinear fractional pantograph delay differential equations whose defining feature is the complete elimination of numerical matrix inversion from the construction of the operational matrices. The technical device is the explicit Baliarsingh–Dutta formula (6), which yields the inverse of the change-of-basis matrix in closed form and in quadratic operations.

First, the attainable accuracy is limited only by floating-point round-off, not by the conditioning of the basis. Across seven problem classes, the method reaches errors of 10^{-13} to 10^{-15}, whereas the Bernoulli, Chebyshev, and Legendre methods stagnate between 10^{-7} and 10^{-9}. On the nonlinear benchmark of Example 2, the improvement is a factor of 3.5×10^5.

Second, the stability of the collocation system is provable and polynomial. Theorem 5.2 establishes that the condition number grows at most quadratically, in contrast with the exponential growth of the competing bases.

Third, the method is robust and efficient in practice. The Newton solver converges in at most six iterations across all examples, and the iteration count decreases with N.

The approach extends naturally to systems, to multi-term and variable-order operators, and to multiple proportional delays. Future work will address two-dimensional pantograph problems and fractional partial differential equations.

Abbreviations

ECM	Euler–Collocation Method
CGL	Chebyshev–Gauss–Lobatto
FFT	Fast Fourier Transform
CPU	Central Processing Unit
MSC	Mathematics Subject Classification

Author Contributions

Fatemeh Sharafi: Conceptualization, Formal Analysis, Investigation, Methodology, Software, Validation, Visualization, Writing – original draft, Writing – review & editing

Conflicts of Interest

The authors declare no conflicts of interest.

References

[1] R. L. Bagley, P. J. Torvik, A theoretical basis for the application of fractional calculus to viscoelasticity, *J. Rheol.* 27 (1983) 201–210. https://doi.org/10.1122/1.549724

[2] I. Podlubny, *Fractional Differential Equations*, Academic Press, San Diego, 1999. https://doi.org/10.1016/B978-0-12-558840-9.X5000-2

[3] D. Baleanu, K. Diethelm, E. Scalas, J. J. Trujillo, *Fractional Calculus: Models and Numerical Methods*, World Scientific, 2012. https://doi.org/10.1142/8180

[4] R. Metzler, J. Klafter, The random walk's guide to anomalous diffusion, *Phys. Rep.* 339 (2000) 1–77. https://doi.org/10.1016/S0370-1573(00)00070-3

[5] A. Iserles, On the generalized pantograph functional-differential equation, *European J. Appl. Math.* 4 (1993) 1–38. https://doi.org/10.1017/S0956792500000966

[6] G. M. N. Ali, M. A. El-Sayed, et al., Fractional pantograph equations: analysis and numerics, *Chaos Solitons Fractals* 133 (2020) 109645. https://doi.org/10.1016/j.chaos.2020.109645

[7] E. H. Doha, A. H. Bhrawy, D. Baleanu, R. M. Hafez, A new Jacobi rational–Gauss collocation method for numerical solution of generalized pantograph equations, *Appl. Numer. Math.* 77 (2014) 43–54. https://doi.org/10.1016/j.apnum.2013.11.003

[8] A. Saadatmandi, M. Dehghan, A new operational matrix for solving fractional-order differential equations, *Comput. Math. Appl.* 59 (2010) 1326–1336. https://doi.org/10.1016/j.camwa.2009.07.006

[9] M. M. Khader, Numerical solution of nonlinear fractional pantograph equations using Legendre polynomials, *J. Egyptian Math. Soc.* 24 (2016) 265–270. https://doi.org/10.1016/j.joems.2015.07.002

[10] Y. Chen, X. Ke, Y. Wei, Numerical algorithm to solve a class of nonlinear fractional pantograph equations, *J. Comput. Appl. Math.* 339 (2018) 262–275. https://doi.org/10.1016/j.cam.2018.02.031

[11] S. Nemati, P. M. Lima, Numerical solution of nonlinear fractional integro-differential equations, *J. Comput. Appl. Math.* 235 (2011) 393–402. https://doi.org/10.1016/j.cam.2010.06.006

[12] P. Baliarsingh, S. Dutta, On an explicit formula for inverse of triangular matrices, *J. Egyptian Math. Soc.* 23 (2015) 297–302. https://doi.org/10.1016/j.joems.2014.06.001

[13] K. Diethelm, *The Analysis of Fractional Differential Equations*, Springer, Berlin, 2010. https://doi.org/10.1007/978-3-642-14574-2

[14] L. N. Trefethen, *Approximation Theory and Approximation Practice*, SIAM, Philadelphia, 2013. https://doi.org/10.1137/1.9781611975949

[15] J. Shen, T. Tang, L.-L. Wang, *Spectral Methods: Algorithms, Analysis and Applications*, Springer, Berlin, 2011. https://doi.org/10.1007/978-3-540-71041-7

[16] B. Fornberg, *A Practical Guide to Pseudospectral Methods*, Cambridge Univ. Press, 1996. https://doi.org/10.1017/CBO9780511626357

[17] M. H. Heydari, M. R. Hooshmandasl, F. Mohammadi, A. Cattani, Wavelets method for solving systems of nonlinear singular fractional Volterra integro-differential equations, *Commun. Nonlinear Sci. Numer. Simul.* 19 (2014) 37–48. https://doi.org/10.1016/j.cnsns.2013.04.028

[18] A. H. Bhrawy, M. A. Zaky, A method based on the Jacobi tau approximation for solving multi-term time–space fractional partial differential equations, *J. Comput. Phys.* 281 (2015) 876–895. https://doi.org/10.1016/j.jcp.2014.10.055

[19] H. Brunner, *Collocation Methods for Volterra Integral and Related Functional Differential Equations*, Cambridge Univ. Press, 2004. https://doi.org/10.1017/CBO9780511543234

[20] W. M. Abd-Elhameed, E. H. Doha, Y. H. Youssri, New spectral second kind Chebyshev wavelets scheme for solving linear and nonlinear fractional differential equations, *Int. J. Appl. Comput. Math.* 4 (2018) 1–17. https://doi.org/10.1007/s40819-017-0380-y

[21] X. Shi, Y. Chen, et al., Spectral collocation methods for fractional multipantograph delay differential equations, *Lithuanian Math. J.* 64 (2024) 1–22. https://doi.org/10.1007/s10986-023-09614-y

[22] W. M. Abd-Elhameed, M. M. Alsuyuti, New spectral algorithm for fractional delay pantograph equation using certain orthogonal generalized Chebyshev polynomials, *Commun. Nonlinear Sci. Numer. Simul.* 141 (2025) 108479. https://doi.org/10.1016/j.cnsns.2025.108479